Science and Technology Indonesia
e-ISSN:2580-4391 *p*-ISSN:2580-4405
Vol. 7, No. 2, April 2022

Research Paper

The Synthesis of CuO/Polystyrene Nanocomposite Superhydrophobic Layer using The Spin Coating Method

Ratnawulan[1]*, Ahmad Fauzi[1], Sarimai[1]

[1]*Department of Physics, Faculty of Mathematics and Natural Science, Universitas Negeri Padang, Padang, 25131, Indonesia*
***Corresponding Author e-mail: ratnawulan@fmipa.unp.ac.id**

Abstract
This paper shows the synthesis of CuO/Polystyrene(PS) nanocomposite superhydrophobic layer using the spin coating method. The objective of this study was to determine the effect of calcination temperature on the contact angle, morphology, and energy gap of the CuO/PS nanocomposite thin layer. Preparation of copper powder into copper oxide (CuO) nanoparticles using the method of High Energy 3 Dimensional Milling (HEM-3D) for 20 hours. The calcination temperature variations used were 100°C , 150°C, 180°C, 200°C, and 300°C. In this study, sample analysis was performed using X-Ray Diffraction (XRD), Scanning Electron Microscopy (SEM), and Ultraviolet-Visible (UV-Vis) Spectrophotometry. The contact angle was determined using the sessile drop method. The findings indicate that the calcination temperature affects the contact angle of the nanocomposite thin films the highest contact angle was obtained at 162° at a temperature of 200°C. The results of SEM analysis obtained that at a temperature of 200°C, the particle size was 62.91 nm and the particles were evenly distributed in the composite layer. The energy gap at 200°C is 2.03 eV. We found that CuO/PS synthesized at a temperature of 200°C was superhydrophobic.

Keywords
Copper Oxide, Calcination Temperature, Contact Angle, an Energy Gap

Received: 30 October 2021, Accepted: 13 February 2022
https://doi.org/10.26554/sti.2022.7.2.158-163

1. INTRODUCTION

Research related to superhydrophobic layers has recently attracted the attention of researchers around the world. The superhydrophobic coating is created by mimicking phenomena already present in nature such as in lotus leaves. This phenomenon is known as the "lotus effect" (Ye et al., 2020). The lotus leaf surface is superhydrophobic because it can produce a high Water Contact Angle (WCA) to the leaf surface (>150°) (Liu et al., 2020; Sabbah et al., 2016; Zhang et al., 2019a).

The superhydrophobic coating has self-cleaning capabilities. Therefore, superhydrophobic materials are widely applied in various fields, including construction (glass and high-rise building paint), automotive (superhydrophobic car paint), biomedical equipment, transportation (anti-corrosion surfaces for space transportation), and solar panels (Huang et al., 2017; Vidal et al., 2019; Zhang et al., 2019b; Yao et al., 2018; Liu et al., 2016).

The hydrophobic surface refers to the lotus leaf mechanism. The superhydrophobic nature of lotus leaves is influenced by two factors, namely the roughness of the nano-micro order and the chemical composition of the surface (Celia et al., 2013; Simpson et al., 2015; Guan et al., 2018). One of the successful superhydrophobic surfaces is using fluorocarbon compounds or -CF_3 groups (such as 1,1,2,2, tetrahydrodesyltrimethoxysilane). However, these compounds have negative effects on the environment such as pollution, as well as toxicity to the environment (Sun et al., 2018). Therefore, in the hydrophobic coating fabrication technology, the use of non-fluorocarbon compounds is preferred because it is environmentally friendly and the price is more affordable (Anitha et al., 2018).

Radwan et al. (2018) have made a superhydrophobic coating using a combination of Al_2O_3 with polystyrene as a hydrophobicity inductor for glass substrates which can produce a superhydrophobic surface with a water contact angle of up to 155°. Xu et al. (2012) succeeded in modifying the hydrophobic surface by using a combination of MnO_2 particles with polystyrene which produces a hydrophobic layer with a water contact angle of up to 155°. Polystyrene is proven to be able to replace fluorinated compounds as hydrophobic agents.

Li and Wang (2010) have successfully synthesized a superhydrophobic coating using a mixture of CuO and fluoroalkylsilane. The resulting contact angle is 162°. Latthe et al. (2015) also synthesized CuO nanocomposites with polysiloxane compounds to produce a hydrophobic layer. The resulting contact

angle is 154°. This information indicates that CuO can be used as a filler for polymer matrix composites to make hydrophobic coatings.

CuO is one of the two stable oxides of copper, the other being Cu_2O. As a mineral, it is known as tenorite. This compound is a product of copper mining in nature. The self-cleaning properties of the CuO surface can be obtained through two photocatalytic and hydrophobic activities (Ratnawulan et al., 2021). CuO metal is a p-type semiconductor with a narrow bandgap energy of 1.9-2.1 eV. CuO can absorb visible light to UV light. This ability is superior to TiO_2, ZnO, SiO_2, and Fe_2O_3 which only absorbs UV light (Wang et al., 2011).

Sarimai et al. (2019) had previously obtained the optimum concentration of CuO in the synthesis of superhydrophobic layers of CuO/PS. The optimum concentration is 1 M. However, the optimum temperature is not known. This optimum temperature information is important for the manufacture of further superhydrophobic coatings. This article explains the procedure for making hydrophobic coatings on glass substrates using CuO nanoparticle fillers reduced from natural copper in West Sumatra and using a polystyrene matrix as a hydrophobic inductor. The synthesis was carried out at various calcination temperatures to see the effect on the contact angle, surface morphology, and energy gap of the CuO/PS nanocomposite thin film.

2. EXPERIMENTAL SECTION

2.1 Materials

The materials used in this study were CuO, acetic acid (CH_3COOH), ethylene glycol ($C_2H_6O_2$), and distilled water and acetone. Copper samples used for making CuO came from Pinti Kayu in Koto Parik Gadang Sub-District, Ateh, South Solok. Preparation of CuO from copper samples following the procedure from previous studies (Ratnawulan et al., 2017). Acetic acid is Water contact angles with the composite coating were taken using a NIKON D5200 camera with the sessile drop method with volume 0.01 mL, a microsyringe at 25 used as a reagent in the formation of precursors. Ethylene glycol is used as a reagent in the formation of CuO gel. The material used as a substrate is glass which is washed using distilled water and acetone, to prevent impurities and fat particles to stick then reducing the evenness of the layer later.

2.2 Methods

2.2.1 Copper Oxide Nanoparticle Preparation

Copper oxide nanoparticle powder was made with the method of High Energy 3 Dimensional Milling (HEM-3D) for 20 hours using copper powder obtained from a village in Sulit Air, Solok, West Sumatra, Indonesia. The obtained copper oxide concentration was 90.63% (Ratnawulan et al., 2017)

2.2.2 Phase Formation of Hydrophobic Layer

1 M CuO powder was added with 15 mL of tetrahydrofuran (THF) and 1 g of polystyrene. This solution was then stirred with a magnetic stirrer for 60 minutes. The solution was then coated on the surface of the glass substrate using a spin coating at a speed of 1,000 rpm for 15 seconds. Then the layers were dried at room temperature for 30 min and annealed for 60 min. After that, the layer was calcined with variations in calcination temperature of 100°C, 150°C, 180°C, 200°C, and 300°C for 1 h and a heating rate of 3°C/min.

2.2.3 CuO/PS Nanocomposite Layer Characterization

The structure of CuO/PS was analyzed by using an X-Ray Powder Diffractometer (XRD, CubiX3Cement); with a long wave of Cu-Kα radiation (λ = 1.5406°A). The composite coating was placed on the holder provided and the resulting diffraction pattern was recorded. Characterization of surface structure and grain size used Scanning Electron Microscopy (SEM) type INSPECT-S50. Measurement of the contact angle between the fluid and the surface of the test material using the sessile drop method and J image software. Measurement of Water Contact Angles (WCA) using the sessile drop method. An amount of 0.01 mL of water was dripped onto the composite layer using a microsyringe at room temperature. Then the water droplets on the layer were photographed using a NIKON D5200 camera. The UV-Vis Spectrophotometer (GENESYS 10S) is used to determine the gap energy value of the CuO/PS thin layer.

2.2.4 Data Analysis

To determine the fasa and structure using High Score Plus software with ICDD (International Center for Diffraction Data) database. Determination of the contact angle using image-J software (V 1.5, National Institutes of Health, Bethesda, MD 20814, USA). The particle size was analyzed using the method of Wienke et al. (1995). Determination of optical band gap energy using the Tauc plot method. This method begins by determining the maximum and minimum transmittance values of the CuO/PS layer obtained from measurements using a UV-Vis Spectrophotometer.

3. RESULT AND DISCUSSION

The X-Ray Diffraction pattern was produced from the CuO/PS nanocomposite layer with calcination temperature variations of 100°C, 150°C, 180°C, 200°C, 300°C can be seen in Figure 1.

Figure 1 shows two significant peaks of intensity at the diffraction angles (2θ) 35.4° and 38.8° (ICDD, No. 00-048-1548). These diffraction angles are the property of CuO compounds. The magnitude of the relative intensity of the series of peaks depends on the number of atoms or ions present and their distribution within the unit cell of the material being tested. The diffraction pattern of each crystalline solid is very typical, which depends on the crystal lattice, the parameter unit, and the wavelength of the X-Ray used.

3.1 Effect of Calcination Temperature on Contact Angle

Figure 2 shows the effect of calcination temperature on the contact angle of the CuO/PS thin layer.

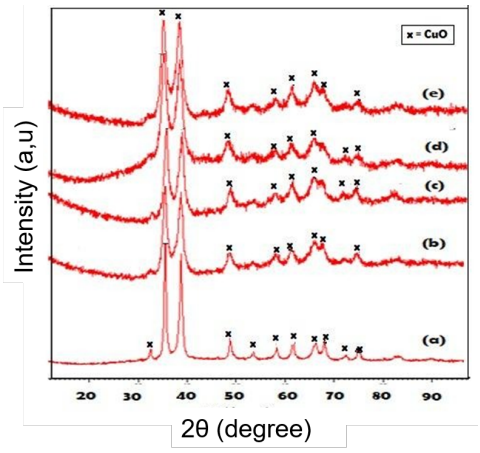

Figure 1. Diffraction Patterns of CuO/PS Nanocomposite Layers with Calcination Temperature Variations of 100°C (a), 150°C (b), 180°C (c), 200°C (d), 300°C (e)

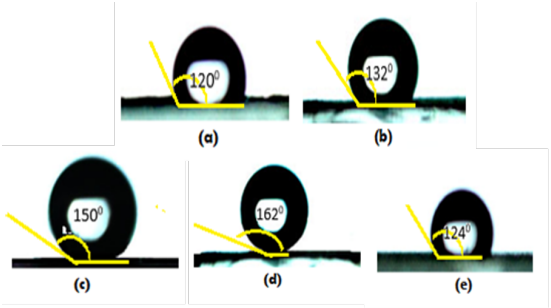

Figure 2. Contact Angles of CuO/PS Nanocomposites with Calcination Temperature Variations of 100°C (a), 150°C (b), 180°C (c), 200°C (d), 300°C (e)

Figure 2 shows the effect of calcination temperature variations of 100°C, 150°C, 180°C, 200°C, and 300°C on the contact angle of the CuO/PS nanocomposite layer. The measurement results show that the highest contact angle is produced at a temperature of 200°C. At a temperature of 200°C the particle size is at the smallest size, namely... nm. From the results of surface structure analysis using SEM, the nano-sized particles are evenly distributed on the surface of the composite coating and contribute to surface roughness. This surface roughness increases the hydrophobic properties of the material. Air is trapped between the surfaces and prevents water from entering the surface. The surface area of the particles that interact with the water becomes smaller. According to the Cassie & Baxter model, the smaller the surface area of the particles interacting with water, the greater the contact angle formed (Zhang et al., 2019a).

3.2 Effect of Calcination Temperature on Morphology of CuO/PS Nanocomposite Layers

The surface morphology of CuO/Polystyrene nanocomposite layers for each variation of calcination temperature 100°C, 150°C, 180°C, 200°C, and 300°C provides information on grain size, grain distribution, and homogeneity of the resulting surface layers. Based on the comparison of SEM imaging results on the surface morphology of each calcination temperature variation, it can be seen the effect of calcination temperature on the morphology of the layers. Figure 3 shows the surface morphology of the CuO/PS layer based on SEM imaging for each calcination temperature at a magnification of 15,000.

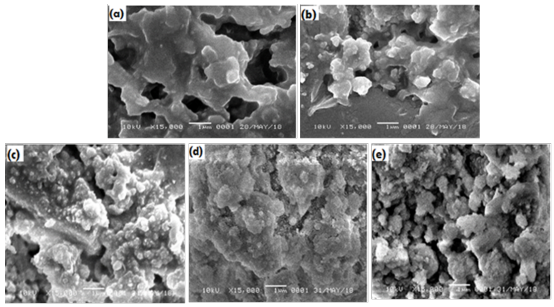

Figure 3. The Results of SEM Imaging Morphology of CuO /Polystyren Nanocomposite Layers with Magnification of 15,000 for Calcination Temperatures 100°C (a), 150°C (b), 180°C (c), 200°C (d), 300°C (e)

Figure 4 shows the surface morphology of the CuO/PS nanocomposite thin layer based on SEM imaging for each calcination temperature with a magnification of 35,000.

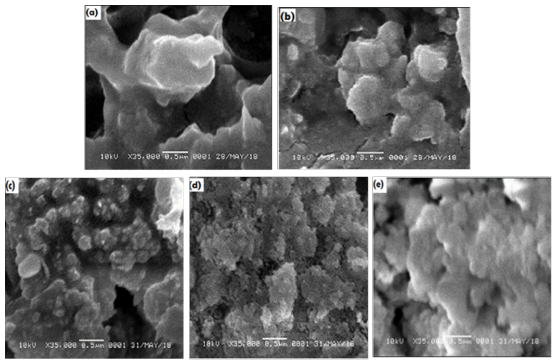

Figure 4. The Results of SEM Imaging Morphology of CuO/PS Nanocomposite Layers with Magnification of 35,000 for Calcination Temperature 100°C (a), 150°C (b), 180°C (c), 200°C (d) and 300°C (e)

Figures 3 and 4 show there are some points of the image have nanocomposite CuO/PS is not yet transformed perfectly. Based on SEM imaging results, the average grain size for temperature variations of 100°C, 150°C, 180°C, 200°C, and 300°C are 31.77 nm, 40.78 nm, 48.91 nm, 50.58 nm, 62.91 nm, and 78.35 nm. Based on the study results obtained the effect of calcination temperature on the grain size of CuO /PS and the contact angle between the fluid and the surface of the layer. The relationship between the three variables can be

seen in Figure 5.

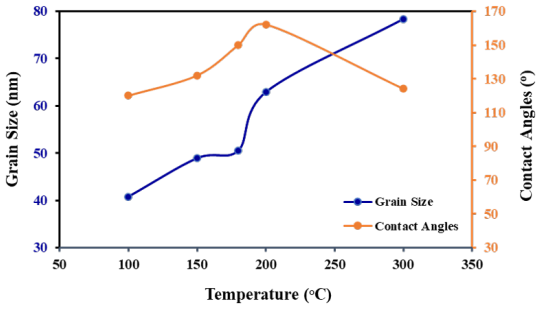

Figure 5. Graph of Temperature Calcination Relationship to Grain Size and Contact Angles

Figure 5 shows that the grain size value of CuO particles when the temperature improves, the contact angle value will improve, except at temperature 300°C the contact angle decline. The same thing happens with grain size, as the temperature is increased the grain size increases with improving temperature. This occurs because of the evaporation of the solution used in dissolving CuO/PS so that it is polar and increases the roughness of the surface. This factor affects the level of surface wetness so that it is superhydrophobic. Therefore, there will be attractions between surface molecules and H_2O molecules which are also polar. The coating of hydrophobic material can modify the surface, making the substrate tend to be nonpolar. There was a significant change in the contact angle on the nanocomposite layer due to the calcination temperature treatment. The contact angle increases when calcined from 100°C and reaches its highest value at 200°C. However, when the calcination temperature is increased to 300°C, the contact angle decreases.

In the calcination of 200°C, there is a large enough change in the contact angle, which is 162°. This contact angle value is the highest of the other temperatures. This is because there is a process of formation of nanoparticles on the surface of the coating due to heating so that the level of roughness becomes high. When the coating is heated using 300°C calcination, the contact angle again drops to 124°. This is because the temperature is too high causing the particles on the surface to start to agglomerate and reduce surface area.

Many protrusions make each particle have high roughness. The protrusions are CuO particles with agglomerated nano order. The hierarchical structure formed in the CuO composite layer/Polystyrene affects the hydrophobicity level. It is due to dropped water on the test surface, air is trapped in the middle of the roughness. Based on the Cassie-Baxter model, the smaller the surface area of the particles that interact with water causes the contact angle formed is greater (Zhang et al., 2019a). This is the cause of the surface being hydrophobic or waterproof. Primary particles begin with electrostatic interactions between CuO molecules and are formed in the nano order. When calcination is high, the particles tend to agglomerate into secondary particles. The particles then *cluster* into larger orders in micro size. However, nanoparticles still form on the *cluster* surface, forming a structural hierarchy.

3.3 Effect of Calcination Temperature on The Energy Gap of CuO/PS nanocomposite Layers

To calculate the value of the energy gap, a graph of the relationship $(\alpha h(c/\lambda))^{1/m}$ with $h(c/\lambda)$ is plotted, then a straight line is drawn from the graph until it intersects the energy axis. Values for direct transition (n = 1/2). The results of the calculation of bandgap optics directly (n = 1/2) to a thin layer of nanocomposite CuO /PS are presented in Figure 6.

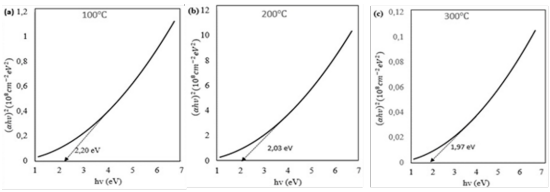

Figure 6. The Energy Gap of CuO/Polystyrene Nanocomposite Layers using The Touch Plot Method with Calcination Temperature Variations 100°C (a), 200°C (b), 300°C (c)

Figure 6 shows the Energy gap value as the plot intersection with hv. The three images show the energy gap of CuO/PS nanocomposite thin layers with calcination temperatures of 100°C, 200°C, and 300°C in order attached in Table 1.

Table 1. The Energy Gap of CuO/PS Nanocomposite Thin Layers

Calcination Temperature (°C)	Energy Gap (eV)
100	2.200
200	2.030
300	1.970

Table 1 shows the value of the energy gap of CuO/Polystyrene nanocomposite layers with calcination temperatures of 100°C, 200°C, and 300°C improve when the temperature is raised. This reduction in the energy gap is consistent with references to similar treatments by Wang et al. (2011). The graph of decreasing energy gap with temperature can be seen in Figure 7.

Figure 7 shows the energy gap increasing with increasing calcination temperature. A thin layer of CuO/PS nanocomposite with a temperature of 300°C has an energy gap that is good enough to be applied as photocatalyst material. The decline of energy gap indicates an improvement of crystals quality that is more regular, the higher the calcination temperature reduces the amorphous phase of the CuO/PS nanocomposite thin layer. The energy gap shift is caused by quantum effects and the presence of amorphous phases in thin layers (Pawar, 2011). The amorphous phase in the thin layer can be reduced

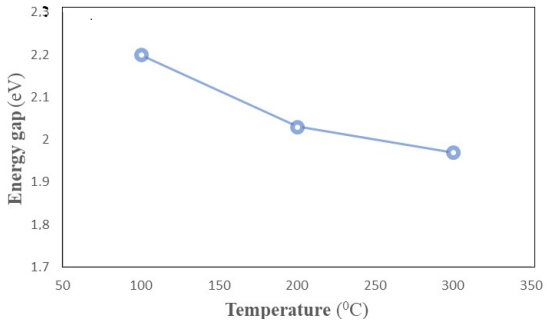

Figure 7. Effect of Temperature on The Gap Energy of CuO/PS Nanocomposite Thin Layers

by improving the calcination temperature to the optimal calcination point. The improvement of calcination gives more energy to the atoms to form crystals.

The samples with variety in calcination at temperatures 100°C to 200°C showed improvement in contact lines with improving temperature. However, when the temperature is 300°C the contact angle formed has decreased. The optimum contact angle is obtained at a calcination temperature of 200°C. The contact angle formed is 162° in the superhydrophobic area. Xu et al. (2012) have made the MnO_2/Polystyrene nanocomposite hydrophobic coating on a copper plate. The results obtained the indication of MnO_2 nanoparticles and calcination temperature affect surface wettability. Xu et al. (2012) have added MnO_2 nanoparticles to improve the hydrophobicity of the polystyrene layer. The basic ingredient used in the study is $MnSO_4.H_2O$ to produce nanoparticles of MnO_2. However, this study did synthesize a hydrophobic layer on a glass substrate by using filler nanoparticles of copper CuO reduced nature of West Sumatra and using matrix polystyrene as a hydrophobic inductor. The findings are expected to have a hydrophobic layer by utilizing the regional natural resources.

Based on the results of SEM characterization, the particle size increases with increasing calcination temperature. However, the particle size is still below the nanometer scale. At a temperature of 200°C, the particle size is more uniform than at other temperatures. This causes the CuO/PS nanocomposite layer at a temperature of 200°C to be superhydrophobic. This is in line with the research of Johan et al. (2011) on the microstructure of thin films which are affected by heating temperature. The grain size growth rate increased more rapidly at higher heating temperatures. The coating prepared without heating has a rough surface and irregular grain size. However, the calcined layer at a temperature of 200°C, the grain size becomes regular and contributes to the hydrophobicity of the material.

In this study, the CuO/Polystyrene nanocomposite layer synthesized at 200°C had superhydrophobic properties. CuO particles and polystyrene molecules accumulate more and more on the surface as the drying temperature increases. However, there was a significant decrease in the contact angle at 300°C. The contact angle obtained at that temperature is 124°. This is thought to be caused by the breaking of the bonds of the CuO nanoparticle composite matrix which is used as a filler due to high temperatures. On the other hand, increasing the calcination temperature reduces the energy gap of the nanocomposite layer. The energy gap of CuO/PS is reduced to 1.97 eV at a temperature of 300°C, so it has the potential to be developed as a photocatalyst material. Further research is needed to ensure that the decrease in hydrophobic properties will be followed by an increase in the photocatalytic properties of semiconductor materials.

4. CONCLUSIONS

This study concludes that calcination temperature affects the value of the contact angle, morphology, and energy gap of CuO/PS nanocomposite thin layers. The addition of calcination temperature affects the contact angle between the water and the surface of the thin layer. The highest contact angle was obtained at 162° at a temperature of 200°C. The addition of temperature affects the morphology of the CuO/PS nanocomposite thin layer, a homogeneous surface formed when the temperature is 200°C. The addition of calcination temperature affects the energy gap, the minimum energy gap obtained at calcination 300°C is 1.97 eV.

5. ACKNOWLEDGEMENT

Thank you to Directorate General of Higher Education (DIKTI), Ministry of Research, Technology and Higher Education, Indonesia, for the Research Grant (Hibah PTM 2019), No. 077/SP2H/LT/DRPM/2019.

REFERENCES

Anitha, C., S. S. Azim, and S. Mayavan (2018). Influence of Particle Size in Fluorine Free Corrosion Resistance Superhydrophobic Coating-Optimization and Stabilization of Interface by Multiscale Roughness. *Journal of Alloys and Compounds*, **765**; 677–684

Celia, E., T. Darmanin, E. T. de Givenchy, S. Amigoni, and F. Guittard (2013). Recent Advances in Designing Superhydrophobic Surfaces. *Journal of Colloid and Interface Science*, **402**; 1–18

Guan, Y., C. Yu, J. Zhu, R. Yang, X. Li, D. Wei, and X. Xu (2018). Design and Fabrication of Vapor-Induced Superhydrophobic Surfaces Obtained from Polyethylene Wax and Silica Nanoparticles in Hierarchical Structures. *RSC Advances*, **8**(44); 25150–25158

Huang, J., S. Wang, and S. Lyu (2017). Facile Preparation of a Robust and Durable Superhydrophobic Coating using Biodegradable Lignin-Coated Cellulose Nanocrystal Particles. *Materials*, **10**(9); 1080

Johan, M. R., M. S. M. Suan, N. L. Hawari, and H. A. Ching (2011). Annealing Effects on The Properties of Copper Oxide Thin Films Prepared by Chemical Deposition. *International Journal Electrochemical Science*, **6**(12); 6094–6104

Latthe, S. S., P. Sudhagar, C. Ravidhas, A. J. Christy, D. D. Kirubakaran, R. Venkatesh, A. Devadoss, C. Terashima, K. Nakata, and A. Fujishima (2015). Self-Cleaning and Superhydrophobic CuO Coating by Jet-Nebulizer Spray Pyrolysis Technique. *CrystEngComm*, **17**(13); 2624–2628

Li, B. and Y. Wang (2010). Facile Synthesis and Photocatalytic Activity of ZnO–CuO Nanocomposite. *Superlattices and Microstructures*, **47**(5); 615–623

Liu, E., H. J. Lee, and X. Lu (2020). Superhydrophobic Surfaces Enabled by Femtosecond Fiber Laser-Written Nanostructures. *Applied Sciences*, **10**(8); 2678

Liu, H., S. W. Gao, J. S. Cai, C. L. He, J. J. Mao, T. X. Zhu, Z. Chen, J. Y. Huang, K. Meng, and K. Q. Zhang (2016). Recent Progress in Fabrication and Applications of Superhydrophobic Coating on Cellulose-Based Substrates. *Materials*, **9**(3); 124

Pawar, S. (2011). Nanocrystalline CuO Thin Films for H_2S Monitoring: Microstructural and Optoelectronic Characterization. *Journal of Sensor Technology*, **1**; 36–46

Radwan, A. B., A. M. Abdullah, A. Mohamed, and M. A. Al-Maadeed (2018). New Electrospun Polystyrene/Al_2O_3 Nanocomposite Superhydrophobic Coatings; Synthesis, Characterization, and Application. *Coatings*, **8**(2); 65

Ratnawulan, A. Fauzi, and S. H. AE (2017). Effect of Calcination Temperature on Phase Transformation and Crystallite Size of Copper Oxide (CuO) Powders. *AIP Conference Proceedings*, **1868**; 060009

Ratnawulan, R., R. Ramli, A. Fauzi, and S. Hayati AE (2021). Synthesis and Characterization of Polystyrene/CuO-Fe_2O_3 Nanocomposites from Natural Materials as Hydrophobic Photocatalytic Coatings. *Crystals*, **11**(1); 31

Sabbah, A., A. Youssef, and P. Damman (2016). Superhydrophobic Surfaces Created by Elastic Instability of PDMS. *Applied Sciences*, **6**(5); 152

Sarimai, Ratnawulan, Yulkifli, and A. Fauzi (2019). Fabrication of Superhydrophobic CuO/Polystyrene Nanocomposite Coating with Variation Concentration. *Journal of Physics: Conference Series*, **1185**(1); 012014

Simpson, J. T., S. R. Hunter, and T. Aytug (2015). Superhydrophobic Materials and Coatings: a Review. *Reports on Progress in Physics*, **78**(8); 086501

Sun, Y., X. Zhao, R. Liu, G. Chen, and X. Zhou (2018). Synthesis and Characterization of Fluorinated Polyacrylate as Water and Oil Repellent and Soil Release Finishing Agent for Polyester Fabric. *Progress in Organic Coatings*, **123**; 306–313

Vidal, K., E. Gómez, A. M. Goitandia, A. Angulo-Ibáñez, and E. Aranzabe (2019). The Synthesis of a Superhydrophobic and Thermal Stable Silica Coating Via Sol-Gel Process. *Coatings*, **9**(10); 627

Wang, G., J. Yang, and Q. Shi (2011). Preparation of Transparent Ultrahydrophobic Silica Film by Sol–Gel Process. *Journal of Coatings Technology and Research*, **8**(1); 53–60

Wienke, D., Y. Xie, and P. K. Hopke (1995). Classification of Airborne Particles by Analytical Scanning Electron Microscopy Imaging and a Modified Kohonen Neural Network (3MAP). *Analytica Chimica Acta*, **310**(1); 1–14

Xu, X., Z. Zhang, F. Guo, J. Yang, X. Zhu, X. Zhou, and Q. Xue (2012). Fabrication of Bionic Superhydrophobic Manganese Oxide/Polystyrene Nanocomposite Coating. *Journal of Bionic Engineering*, **9**(1); 11–17

Yao, C. W., D. Sebastian, I. Lian, Ö. Günaydın-Şen, R. Clarke, K. Clayton, C. Y. Chen, K. Kharel, Y. Chen, and Q. Li (2018). Corrosion Resistance and Durability of Superhydrophobic Copper Surface in Corrosive NaCl Aqueous Solution. *Coatings*, **8**(2); 70

Ye, Y., F. Zeng, M. Zhang, S. Zheng, J. Li, and P. Fei (2020). Hydrophobic Edible Composite Packaging Membrane Based on Low-Methoxyl Pectin/Chitosan: Effects of Lotus Leaf Cutin. *Food Packaging and Shelf Life*, **26**; 100592

Zhang, B., W. Xu, Q. Zhu, S. Yuan, and Y. Li (2019a). Lotus-Inspired Multiscale Superhydrophobic AA5083 Resisting Surface Contamination and Marine Corrosion Attack. *Materials*, **12**(10); 1592

Zhang, Y. P., P. P. Li, P. F. Liu, W. Q. Zhang, J. C. Wang, C. X. Cui, X. J. Li, and L. B. Qu (2019b). Fast and Simple Fabrication of Superhydrophobic Coating by Polymer Induced Phase Separation. *Nanomaterials*, **9**(3); 411

